Studies on the ionospheric region during low solar activity in Brazil

Claudia M. N. Candido

National Institute for Space Research - INPE
Brazil

Plasma Bubbles-Spread-F

OI 630.0-nm
Peak at 250 km - F-layer bottomside

OI 777.4-nm
Peak at 350 km - F-layer peak

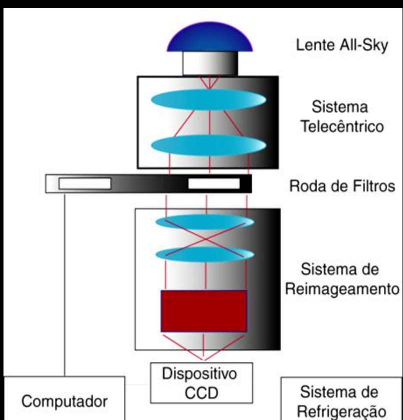

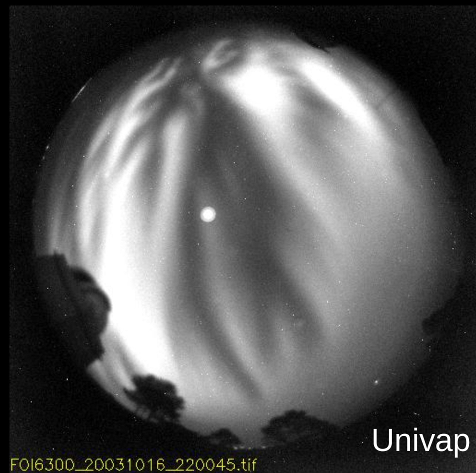

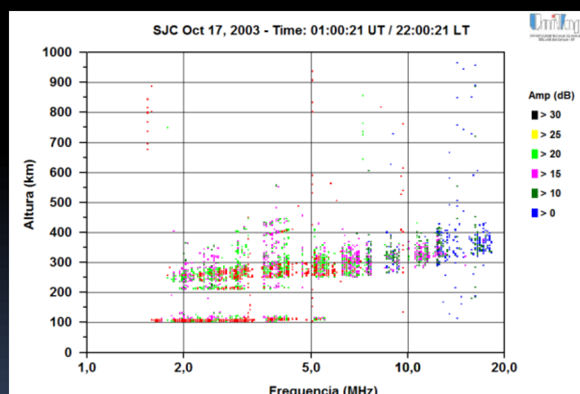

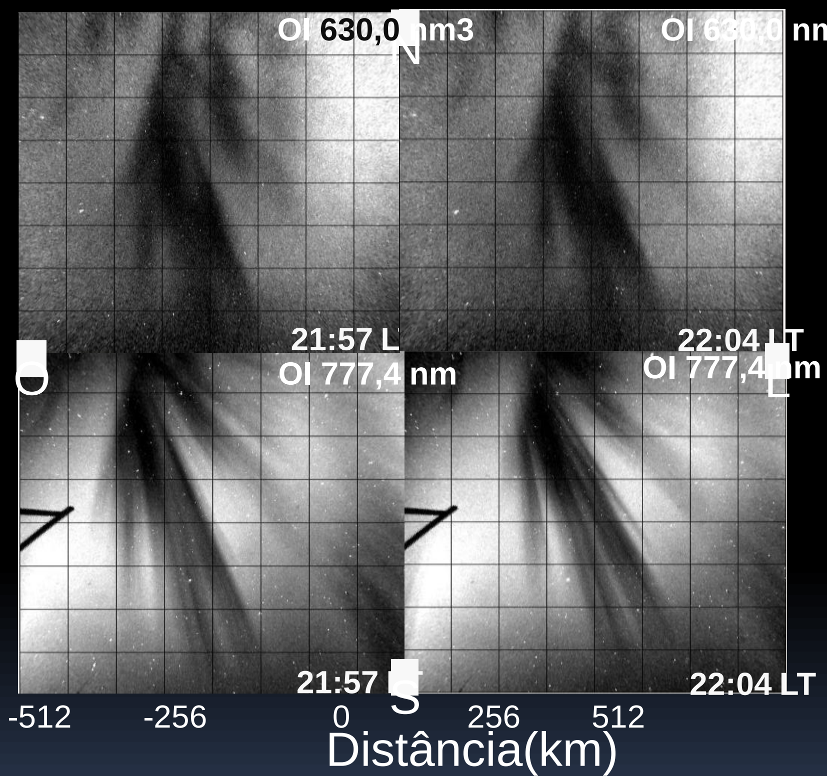

OI 7774.0-nm - Fine structures

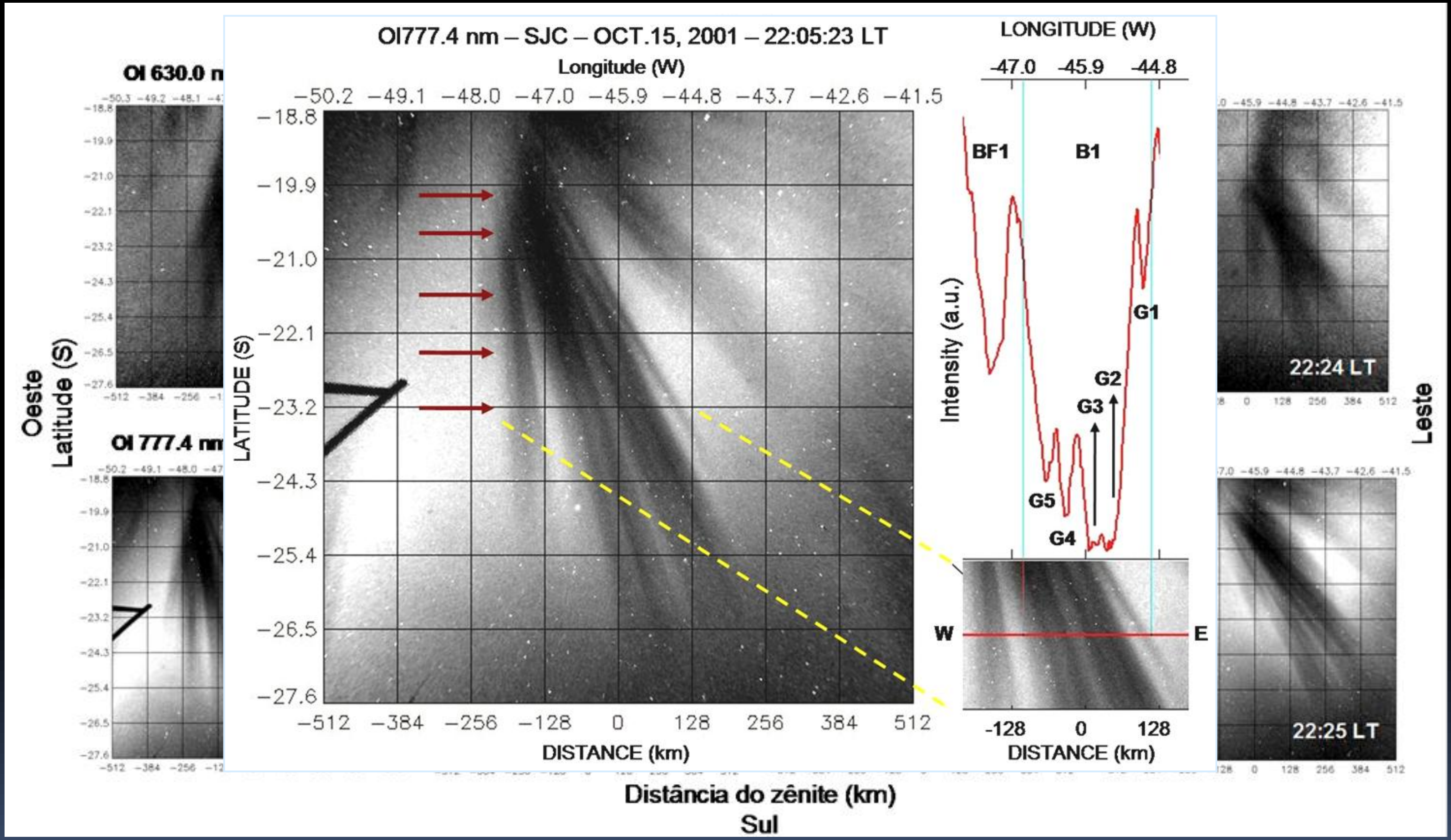

Distúrbios ionosféricos propagantes
(*TIDs – Traveling ionospheric disturbances*)

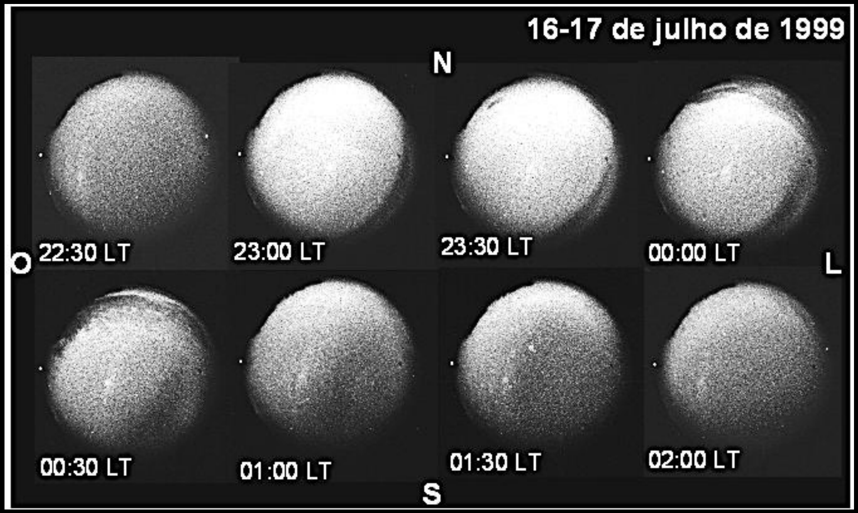

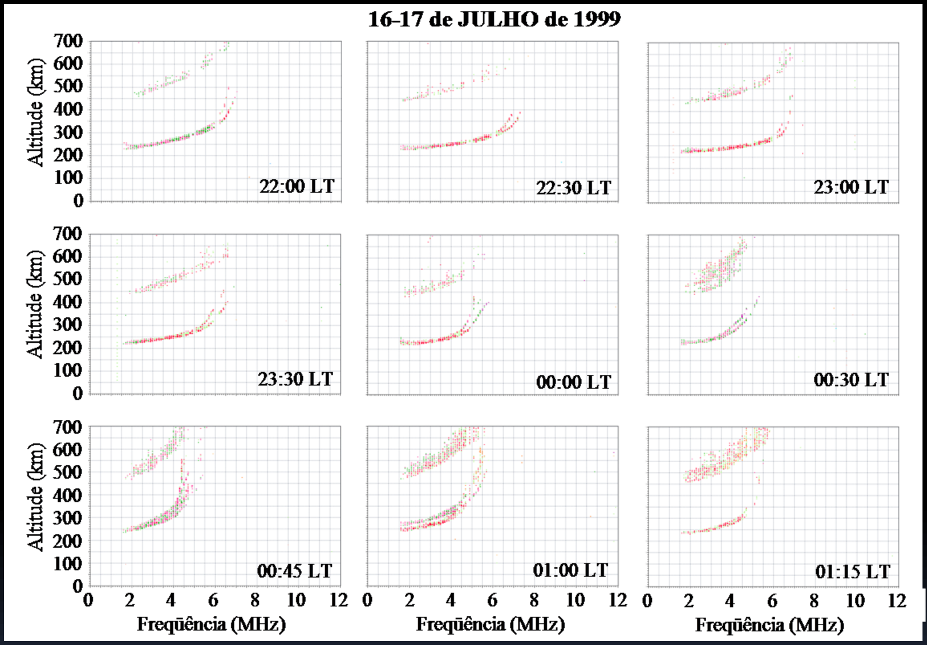

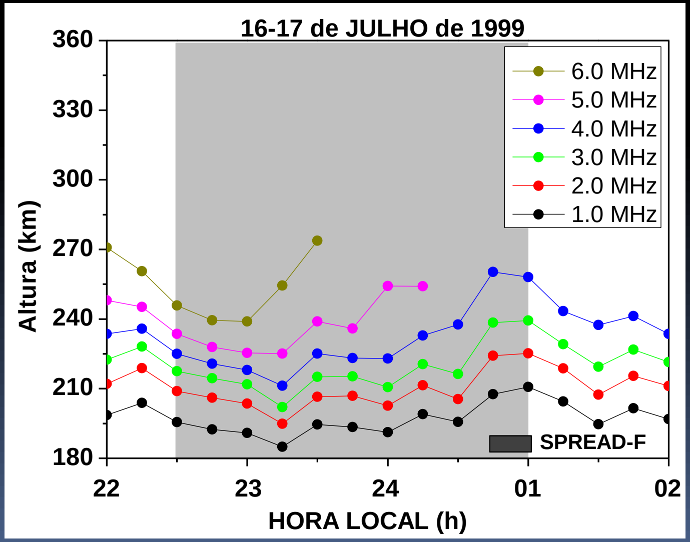

Solar minimum of the solar cycle 23-24 2008-2009

What happened?

Previous solar minima
1966, 1976,1986, 1996 $\Rightarrow$ 2006

Observed
2008 $\Rightarrow$ 2 years later!

Unusually deep and complex

266 spotless days in 2008

Magnetic field at the solar poles 40% weaker than previous solar cycles

Months with no sunspots – August 2009

Lower UV radiation emission

Lower solar flux

Lower Total Solar Irradiance (TSU)

Sunspot area as a function of latitude and time

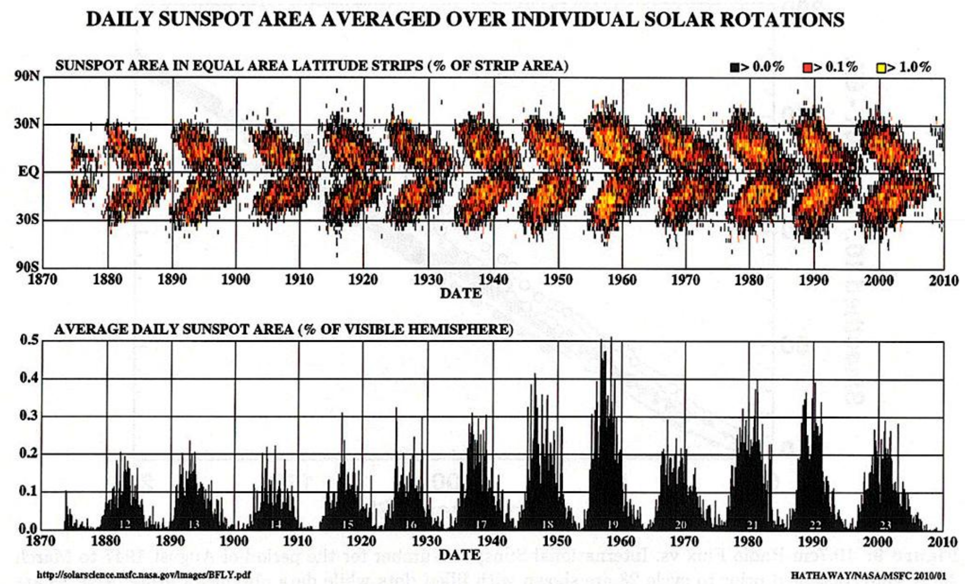

Figure 8: Sunspot area as a function of latitude and time. The average daily sunspot area for each solar rotation since May 1874 is plotted as a function of time in the lower panel. The relative area in equal area latitude strips is illustrated with a color code in the upper panel. Sunspots form in two bands, one in each hemisphere, that start at about 25° from the equator at the start of a cycle and migrate toward the equator as the cycle progresses.

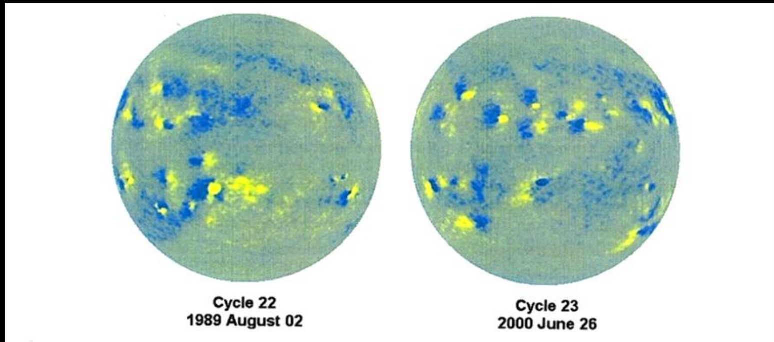

Figure 12: Hale's Polarity Laws. A magnetogram from sunspot cycle 22 (1989 August 2) is shown on the left with yellow denoting positive polarity and blue denoting negative polarity. A corresponding magnetogram from sunspot cycle 23 (2000 June 26) is shown on the right. Leading spots in one hemisphere have opposite magnetic polarity to those in the other hemisphere and the polarities flip from one cycle to the next.

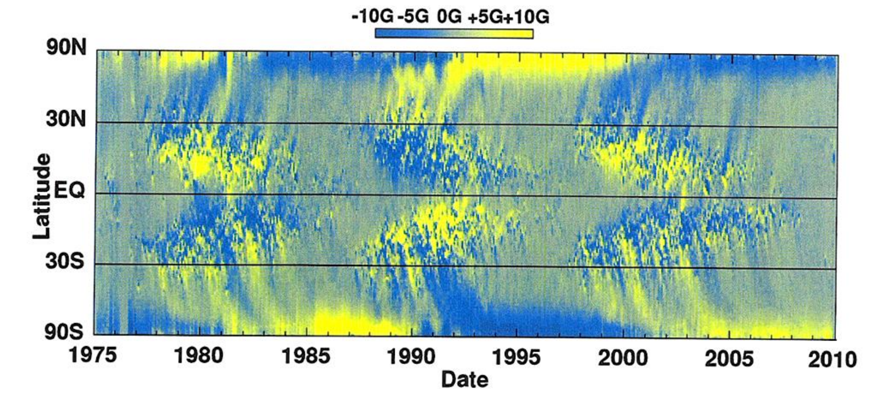

Figure 14: A Magnetic Butterfly Diagram constructed from the longitudinally averaged radial magnetic field obtained from instruments on Kitt Peak and SOHO. This illustrates Hale's Polarity Laws, Joy's Law, polar field reversals, and the transport of higher latitude magnetic field elements toward the poles.

Russel et al., Rev. Geop., 2010

Solar Indexes

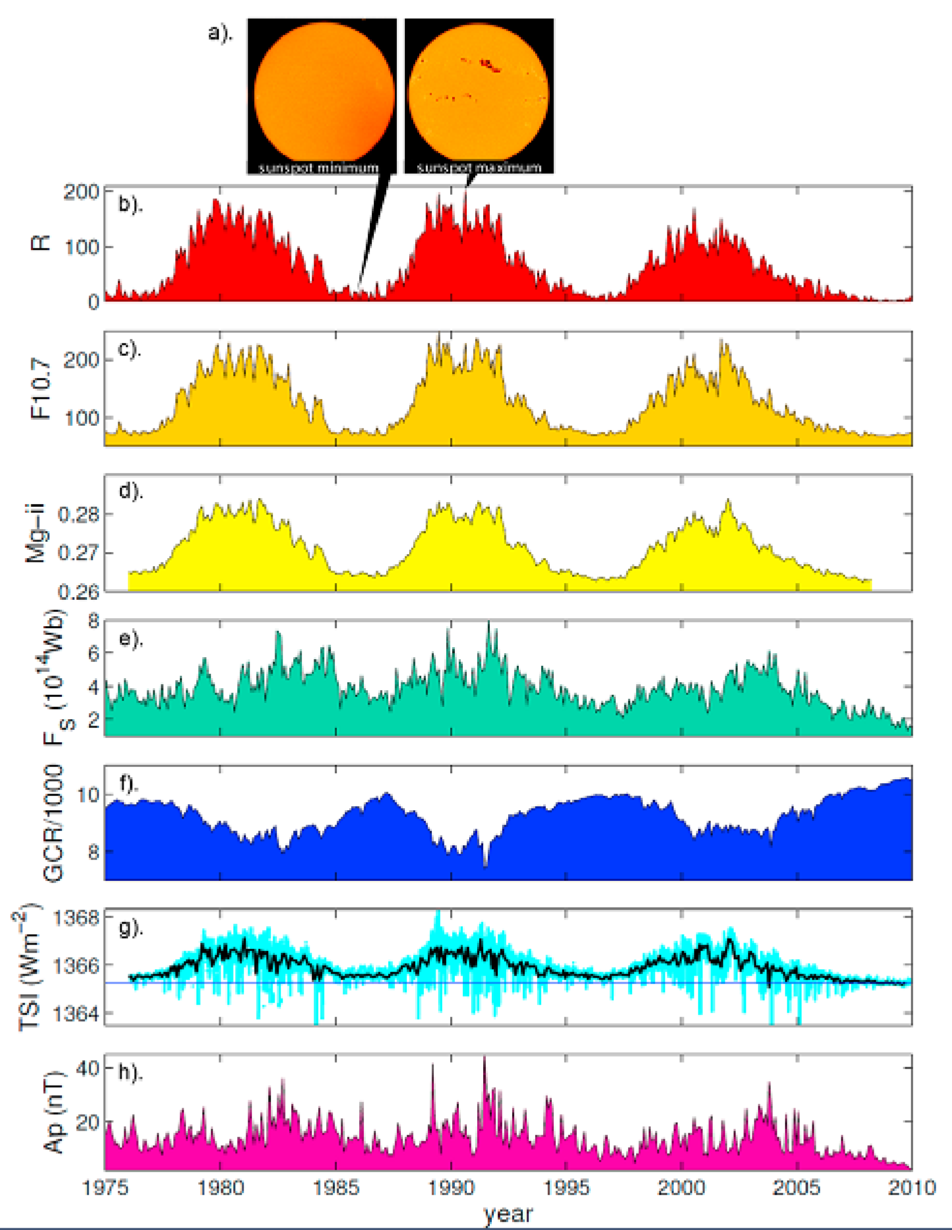

a) Images of the Sun at sunspot max and min
b) Sunspots number
c) F10.7
d) Mg-ii (280 nm) emission intensity
e) Fs – Open solar flux
f) GCR (galactic cosmic rays) – Antarctica
g) TSI (total solar irradiance) – PMOD
h) Ap index

Figure 1. (a) Images of the Sun at sunspot minimum and sunspot maximum. Observed variations of (b) the sunspot number R (a dimensionless weighted mean from a global network of solar observatories, given by $R = 10N + n$, where N is the number of sunspot groups on the visible solar disk and n is the number of individual sunspots); (c) the 10.7 cm solar radio flux, $F_{10.7}$ (in W m^{-2} Hz^{-1}, measured at Ottawa, Canada); (d) the Mg ii line (280 nm) core-to-wing ratio (a measure of the amplitude of the chromospheric Mg II ion emission, which on time scales up to the solar cycle length has been found to be correlated with solar UV irradiance at 150–400 nm); (e) the open solar flux F_S derived from the observed radial component of interplanetary field near Earth; (f) the GCR counts per minute recorded by the neutron monitor at McMurdo, Antarctica; (g) the PMOD composite of TSI observations; and (h) the geomagnetic Ap index. All data are monthly means except the light blue line in Figure 1g, which shows daily TSI values. (Updated from *Lockwood and Fröhlich* [2007].)

Gray et al., Rev. Geop. 2010

Solar Indexes

TSI : total Solar Irradiance ($W.m^2$)

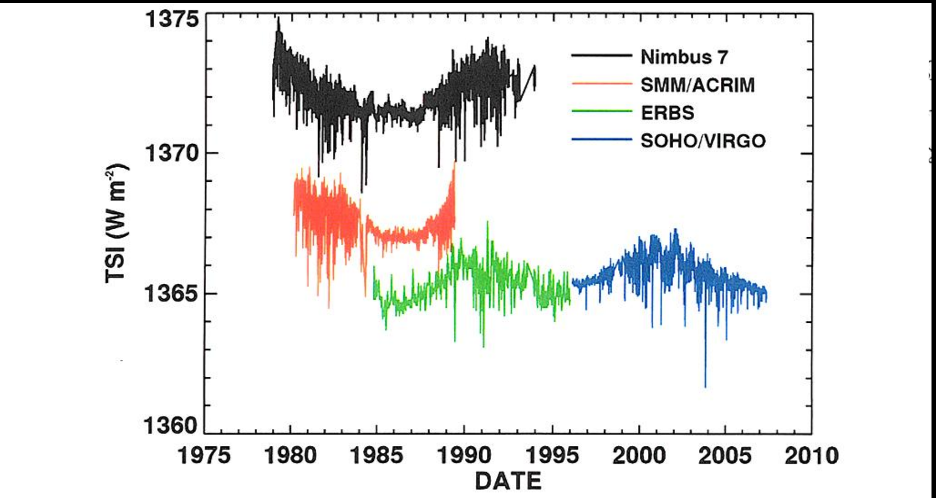

Figure 10: Daily measurements of the Total Solar Irradiance (TSI) from instruments on different satellites. The systematic offsets between measurements taken with different instruments complicate determinations of the long-term behavior.

10.7 cm solar flux vs solar SSN

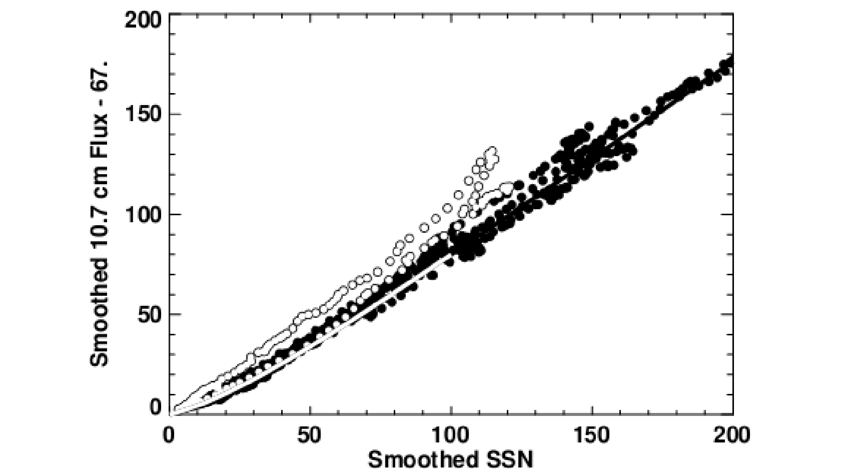

Figure 9: 10.7cm Radio Flux vs. International Sunspot Number for the period of August 1947 to March 2009. Data obtained prior to cycle 23 are shown with filled dots while data obtained during cycle 23 are shown with open circles. The Holland and Vaughn formula relating the radio flux to the sunspot number is shown with the solid line. These two quantities are correlated at the 99.7% level.

TSI

Radiant energy emitted by the Sun at all wavelenghts crossing a square meter each second outside the Earth's atmosphere

Hathaway, Living Rev. S. Phys., 2010

F10.7

10.7 cm solar flux is the disk integrated emission from the Sun at the λ=10.7 cm (2800 MHz)

$$F^{10.7} = 67 + 0.97R_I + 17.6\,(e^{-0.035RI} - 1)$$

Total Solar Irradiance TSI

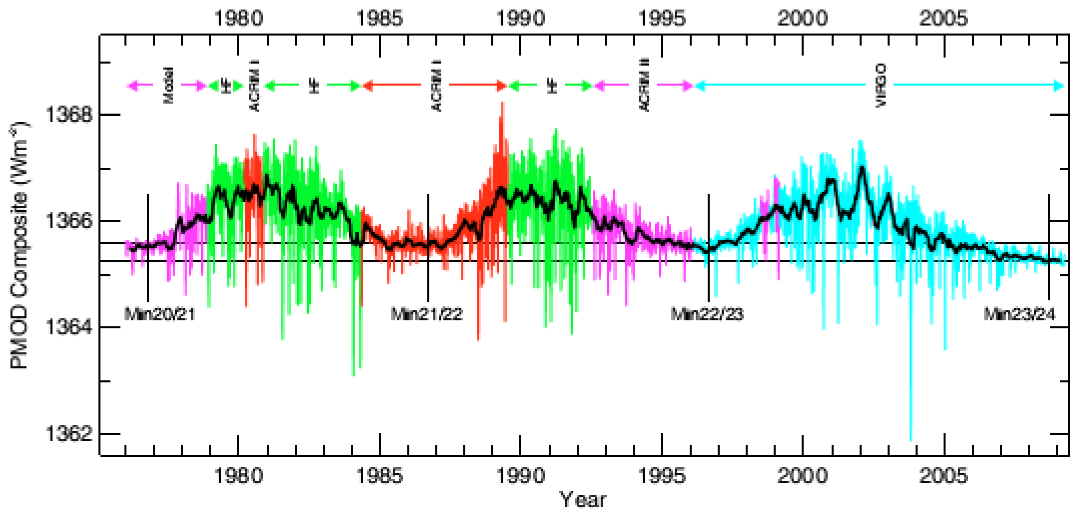

Fig. 1. Daily TSI of the PMOD composite (updated until end of March 2009, Version 41_62_0904) and extrapolated with a proxy model back to 1976. The amplitudes of the three cycles decrease first and then increase again. The two horizontal lines indicate the value of the minima in 1986 and 2008, respectively. Note the low value of the 2008 minimum, which is 0.22 Wm^{-2} lower than the previous one, or 22% in terms of the cycle amplitude.

Frohlich, C., A&A 501, L27–L30 (2009)

TSI was 0.2 Wm^{-2} lower than it was during the last minimum in 1996 (~22%)

TSI is Earth's dominant energy input (10^4 > the next highest energy)

Radiative forcing of climate

Direct impact on sea surface temperatures and hydrological cycles

Galactic Cosmic Rays (GCR)

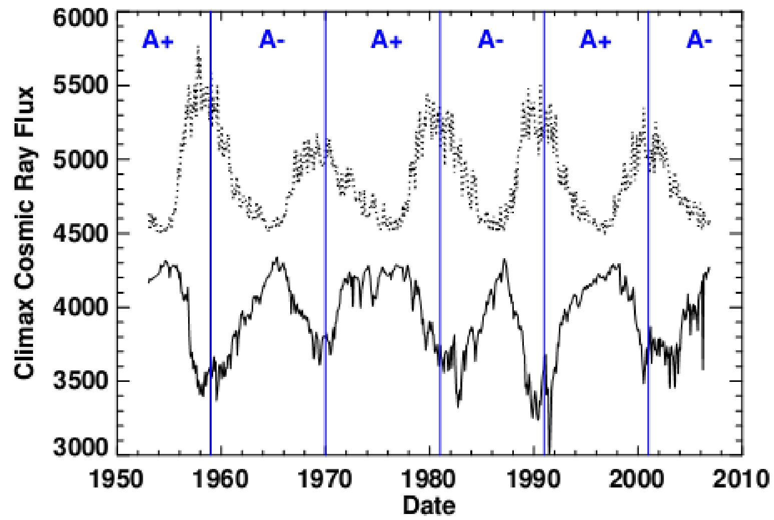

Figure 20: Cosmic Ray flux from the Climax Neutron Monitor and rescaled Sunspot Number. The monthly averaged neutron counts from the Climax Neutron Monitor are shown by the solid line. The monthly averaged sunspot numbers (multiplied by five and offset by 4500) are shown by the dotted line. Cosmic ray variations are anti-correlated with solar activity but with differences depending upon the Sun's global magnetic field polarity (A+ indicates periods with positive polarity north pole while A− indicates periods with negative polarity).

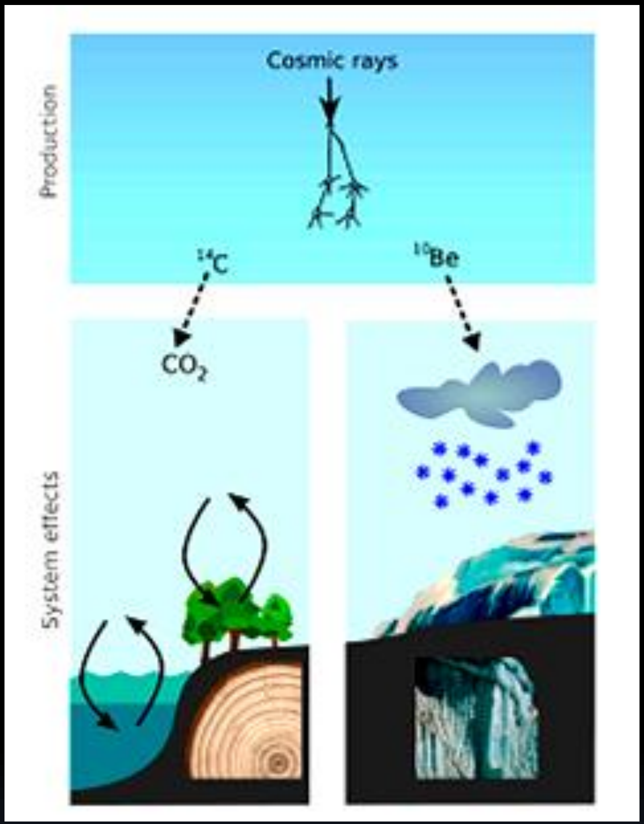

Ionisation on lower atmosphere,
Impact on electric field and on
Condensation nuclei

Steinhilber et al., PNAS, 2012

Forcing factor	Generic mechanism
Total solar irradiance	Radiative forcing of climate Direct impact on sea surface temperatures and hydrological cycle
Solar UV irradiance	Heating the upper and middle atmosphere dynamic coupling down to troposphere. Middle and lower atmosphere chemistry and composition; impacts temperature and radiative forcing
Solar energetic particles	Ionization of upper and middle atmosphere, impact on composition and temperatures. –ionosphere-termosphere coupling
Galactic cosmic rays	Ionisation on lower atmosphere, impact on electric field and on condensation nuclei

Haigh, Living Revies S. Phys., 2007

Solar Minimum Relevance

Associated with lower surface temperatures in the Earth

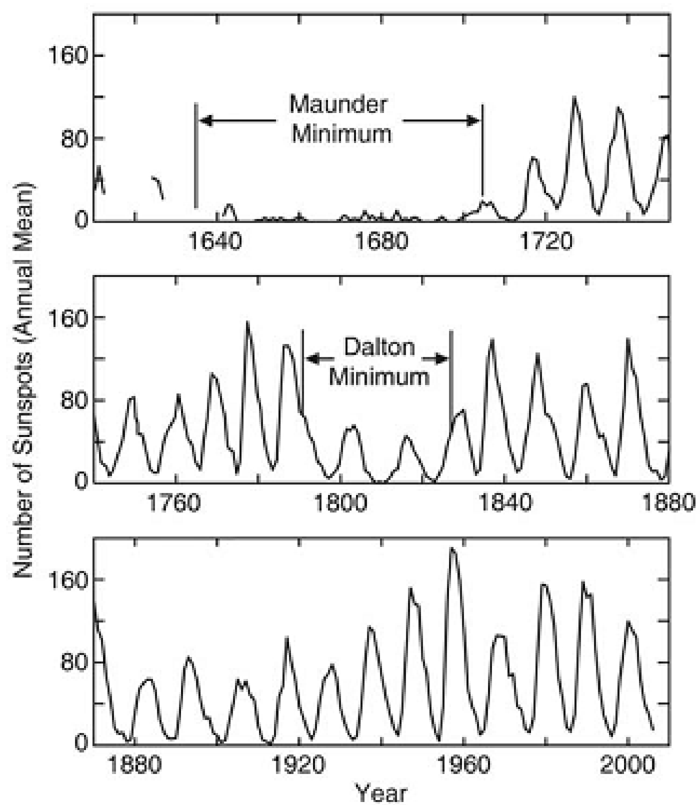

Figure 15. The smoothed annual sunspot number going back to 1605, illustrating the Maunder minimum and the Dalton minimum.

17 th century

Low temperatures – Europe

Low sunspot number

Low solar activity

Maunder minimum (Eddy, 1976)

Total solar irradiance (TSI)

Solar activity

Earth's Climate

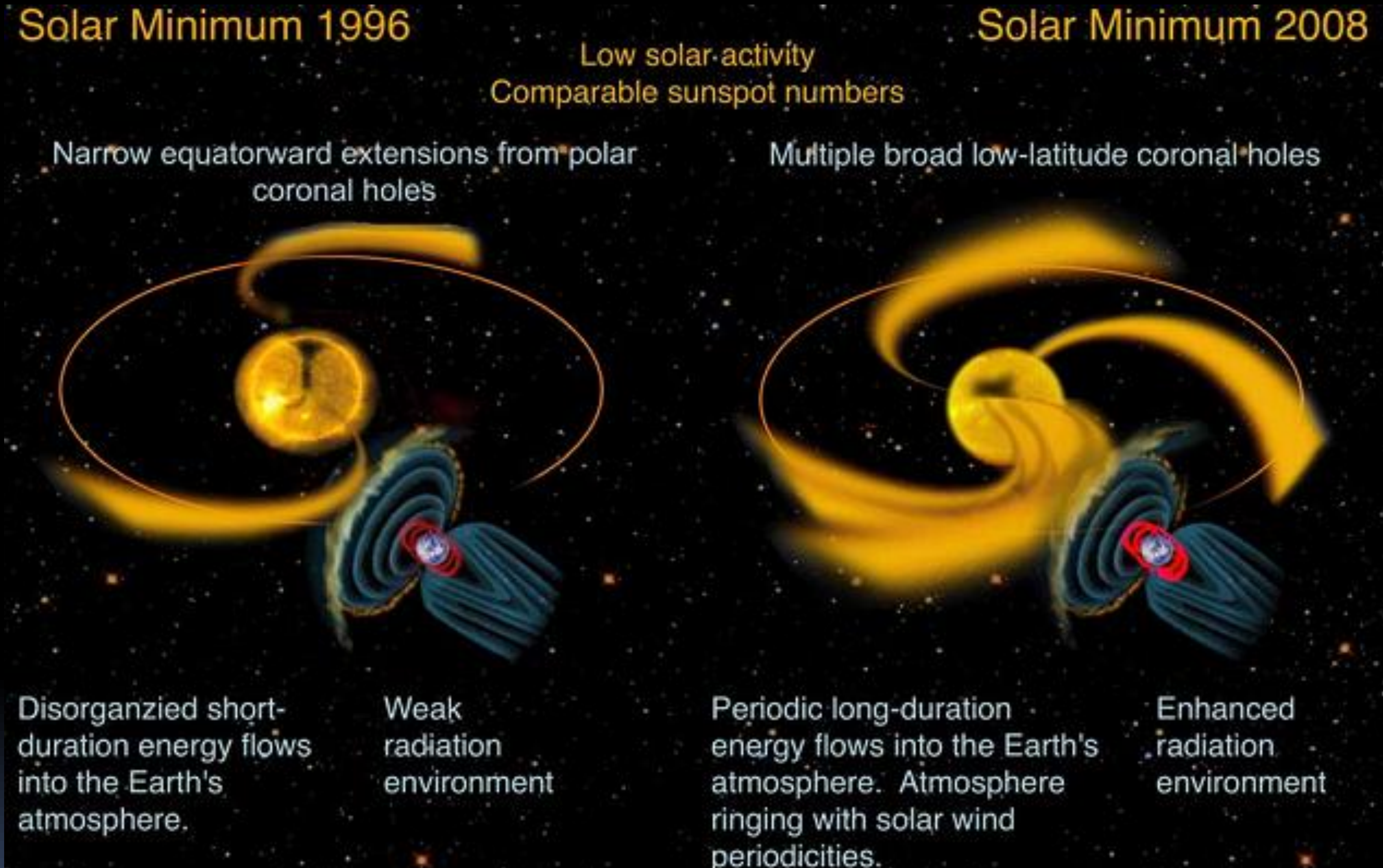

Gibson, JGR., 2009

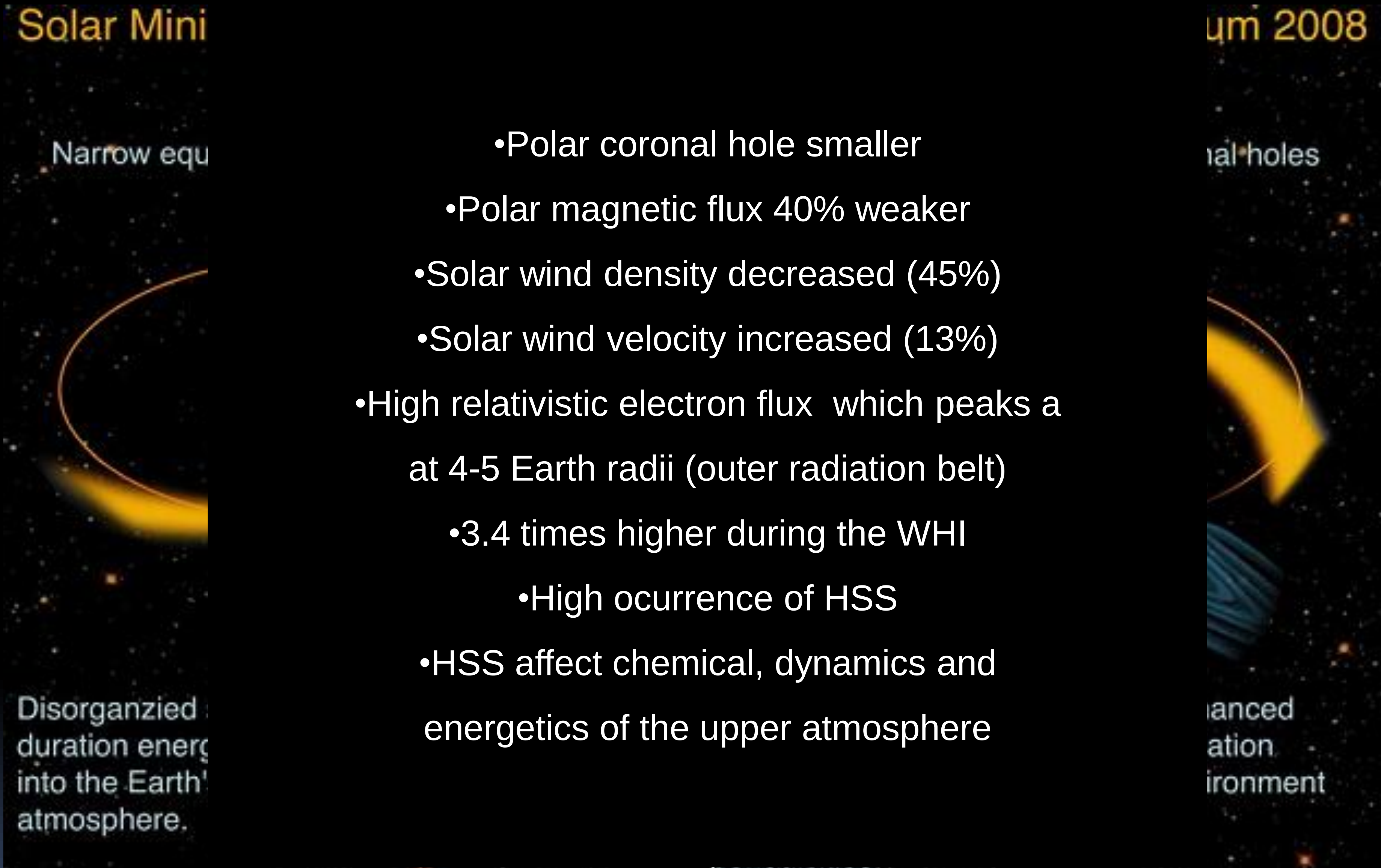

- Polar coronal hole smaller
- Polar magnetic flux 40% weaker
- Solar wind density decreased (45%)
- Solar wind velocity increased (13%)
- High relativistic electron flux which peaks a at 4-5 Earth radii (outer radiation belt)
- 3.4 times higher during the WHI
- High ocurrence of HSS
- HSS affect chemical, dynamics and energetics of the upper atmosphere

Gibson, JGR., 2009

	Solar Maximum	Solar Minimum
Heliospheric magnetic fields	Strong and disorganized	Weak and organized
Ejection of Mass and energy	Higher ocurrence of CMEs e Solar flares	Higher ocurrence of Feixes rápidos (HSS)
Sunspots number	High	Low or null
Galactic Cosmic Rays in the Earth	Shielded by CMEs	Higher penetration ^{10}Be and ^{14}C

Learn more about the Solar Dynamo

Predict next solar cycles

Influence of the Solar activity on Earth's climate

Set instruments

Coupling processes in the upper atmosphere

Global dynamics processes

The ionosphere during the last two solar minimum over the Brazilian region

Claudia M. N. Candido
I. S. Batista

INPE
National Institute of Space Research
Brazil

Solar Minima

1996-1997 and 2008-2009

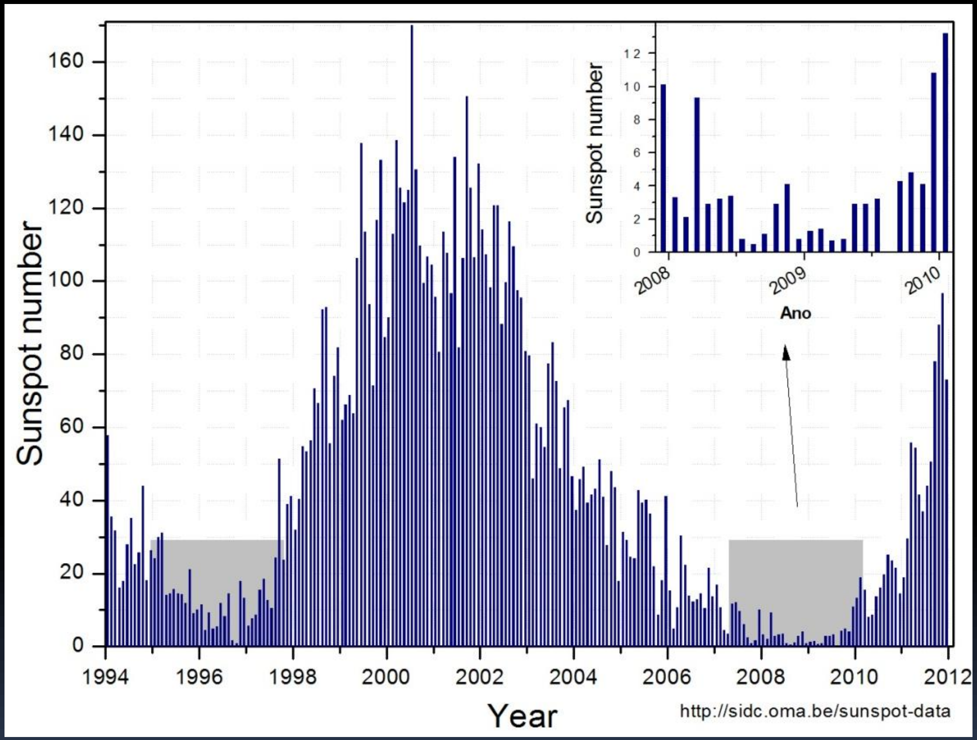

Observations

Low Latitude MSTIDs

Post-Midnight F-region irregularities

Spread-F in ionograms

and Post midnight 5-m irregularities

(RTI maps)

Optical imaging

Digisondes

30 MHz Coherent Backscatter Radar

Observation sites

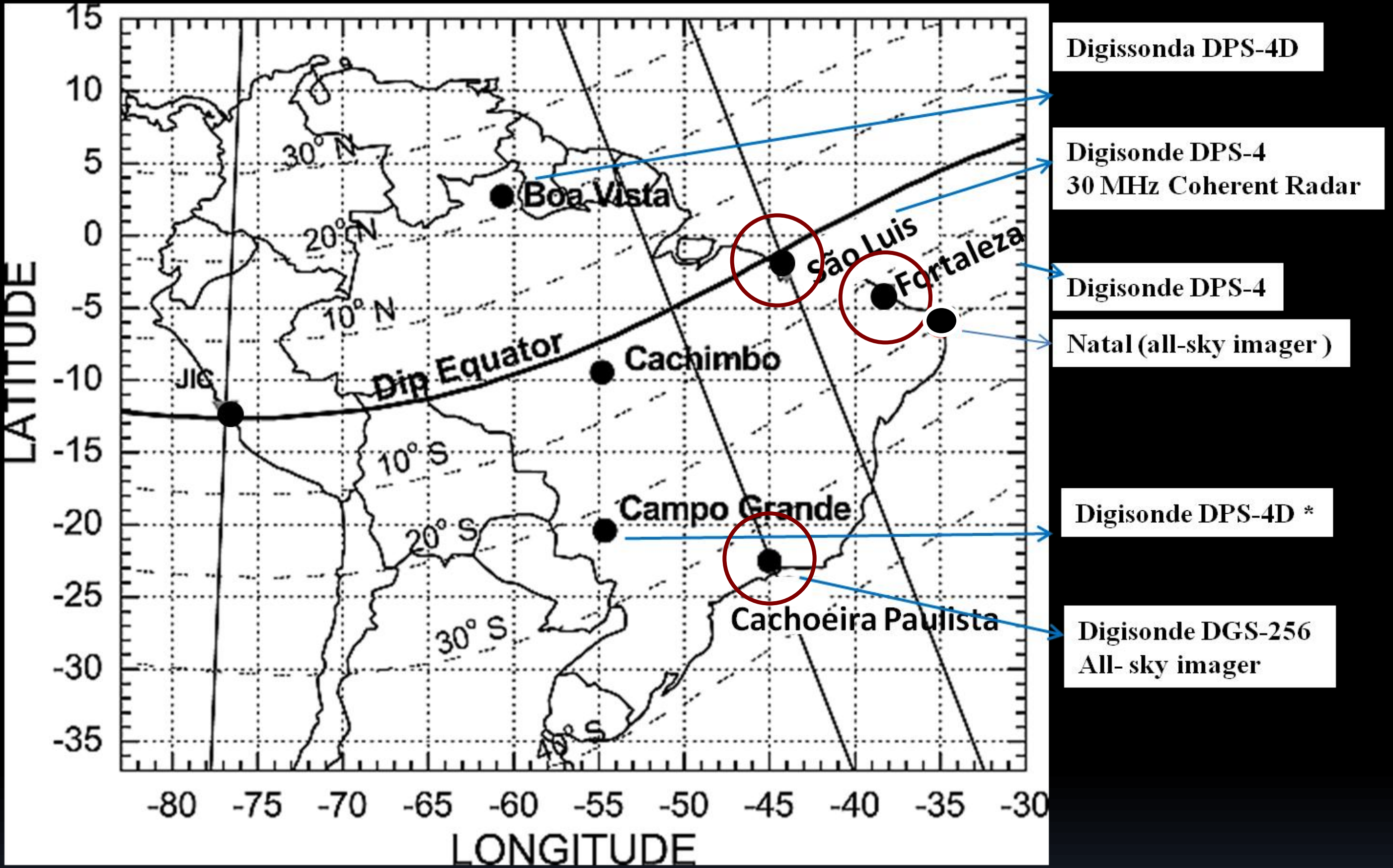

Sao Luis (44.2° W, 2.33° S, dip angle: −6.9°)

Fortaleza (38.45°W, 3.9° S, dip angle: −16°)

Cachoeira Paulista (23º S, 45º W, dip angle: -32)

Low latitude – Cachoeira Paulista 23º S, 45º W

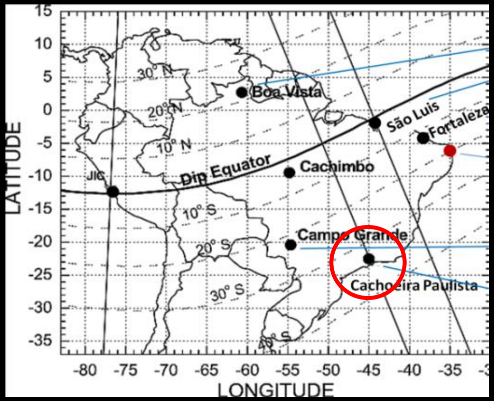

Plasma Bubbles,
Gravity waves
and
MSTIDs
as seen by optical techniques
over
low latitude

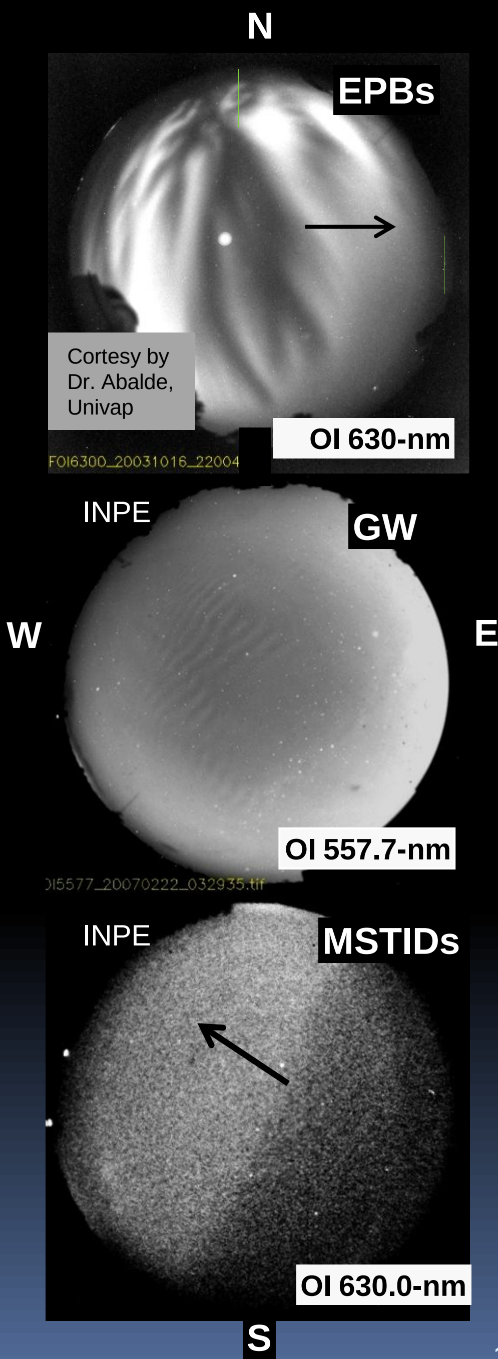

Plasma bubbles vs. MSTIDs
Climatology

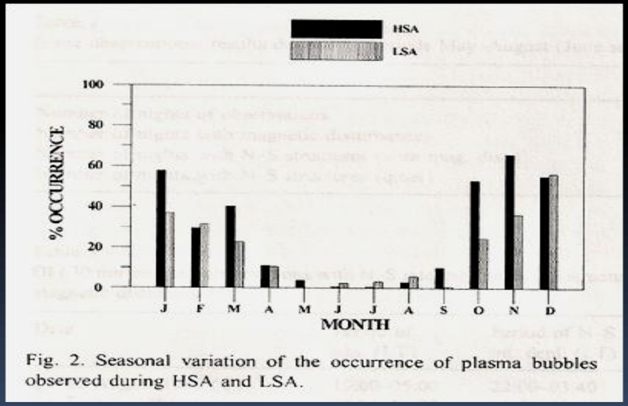

Fig. 2. Seasonal variation of the occurrence of plasma bubbles observed during HSA and LSA.

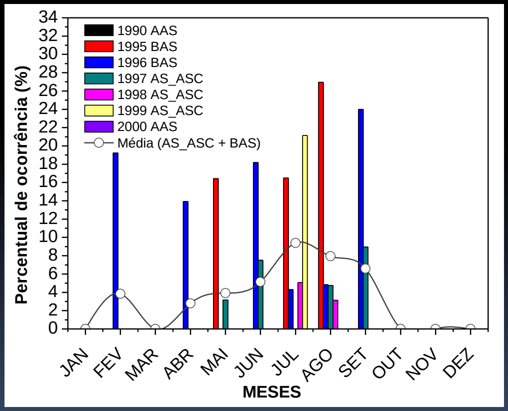

Sahai., JASTP, 2000
Airglow

Candido et al., GRL, 2008
Airglow data

Low latitude – MSTIDs Solar minimum 1996

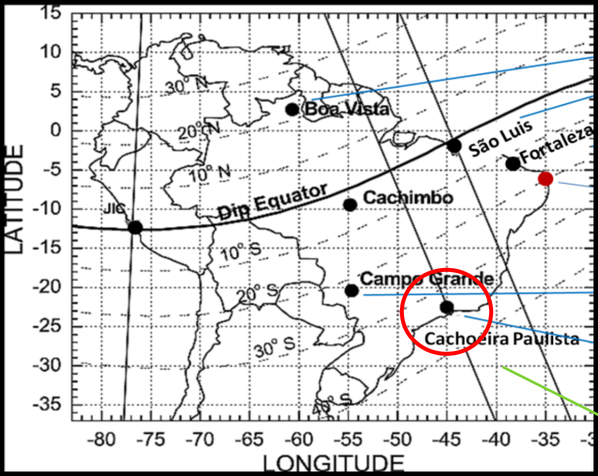

OI 630-nm emission
All-sky imaging system

Candido et al., GRL, 2008

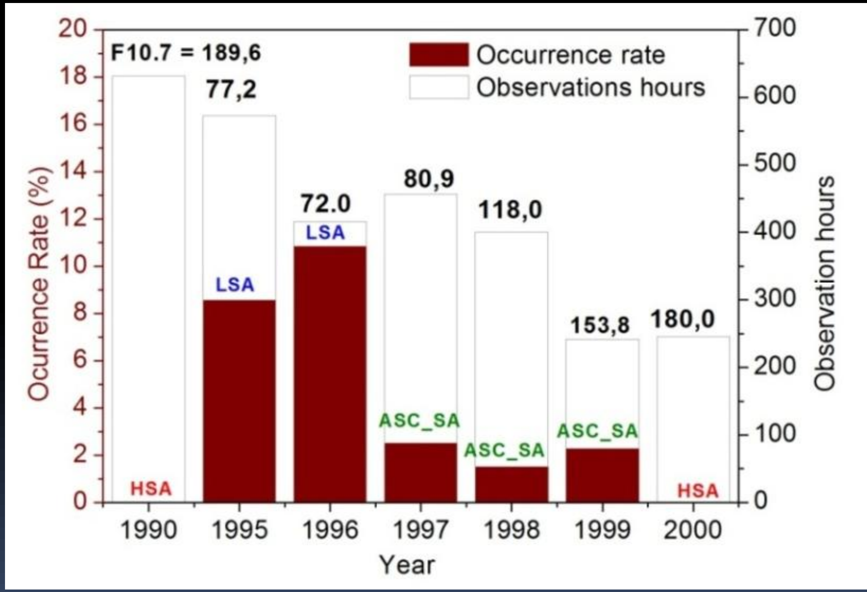

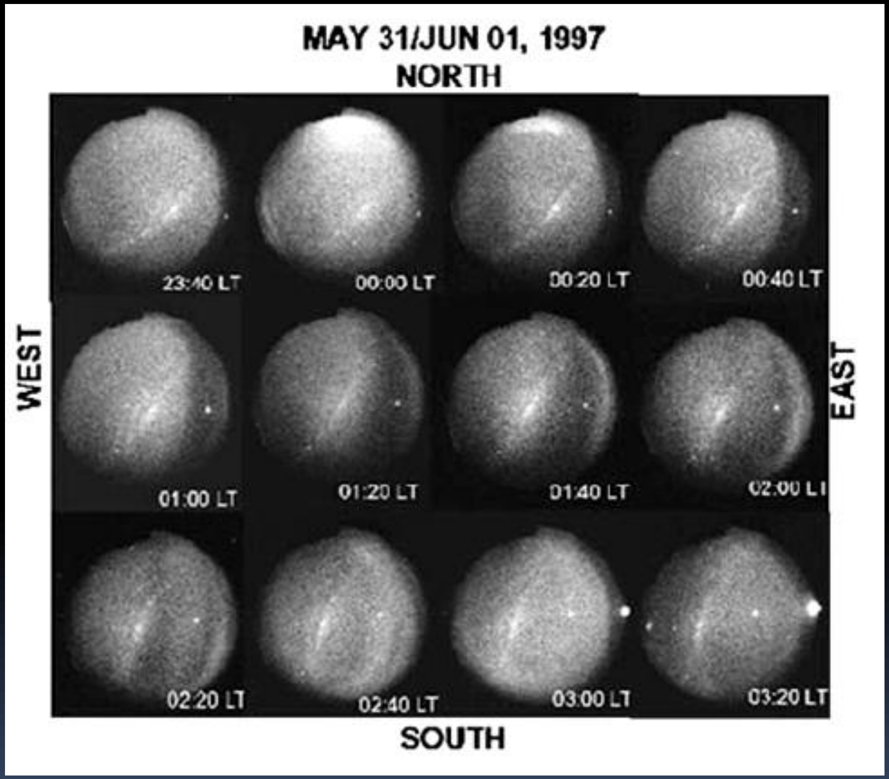

Looking at the ionosphere during the solar minimum 2006!

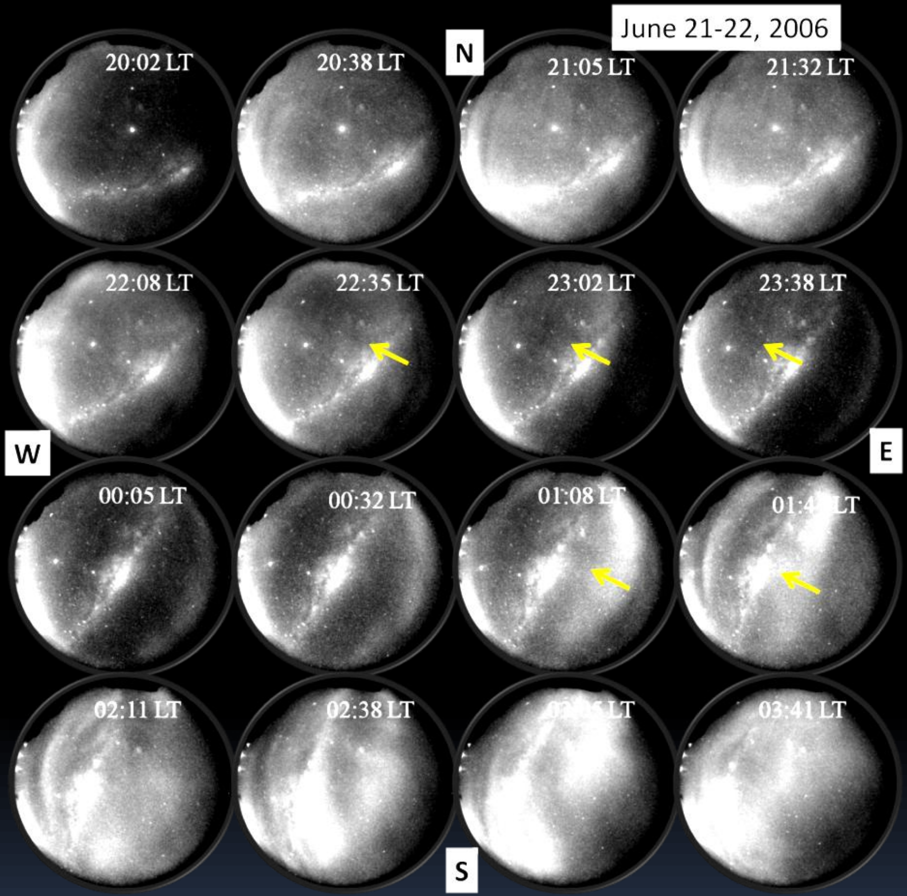

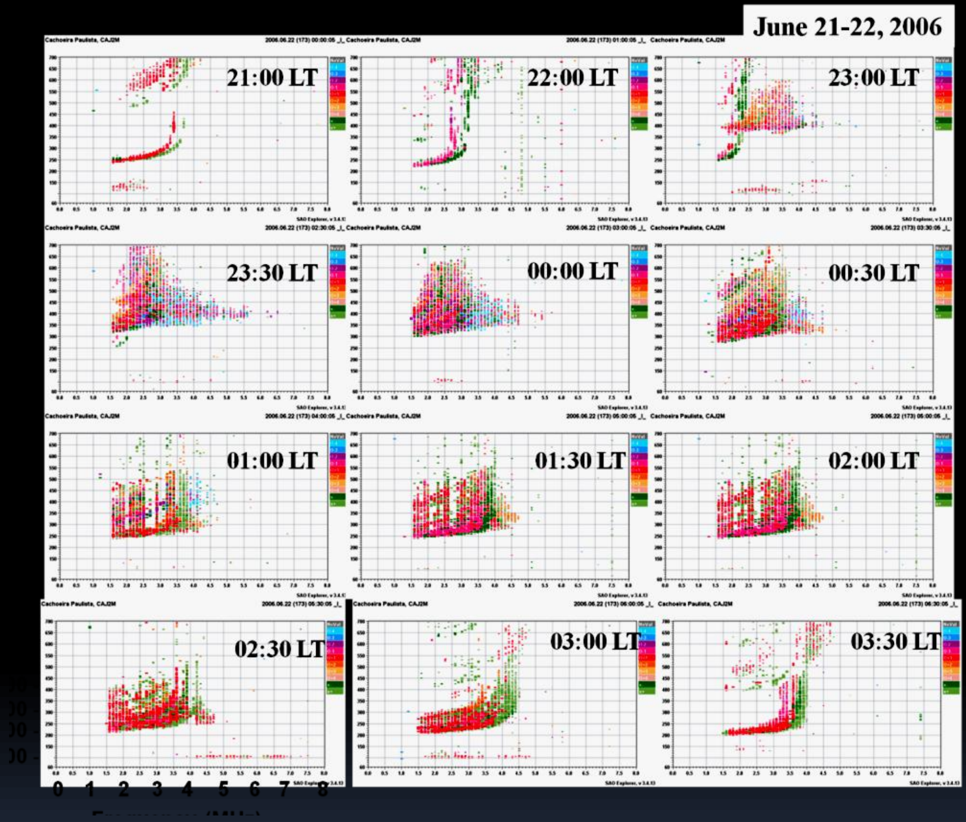

Low latitude MSTIDs and plasma irregularities/spread-F

Looking at the ionosphere in the solar minimum 2007!

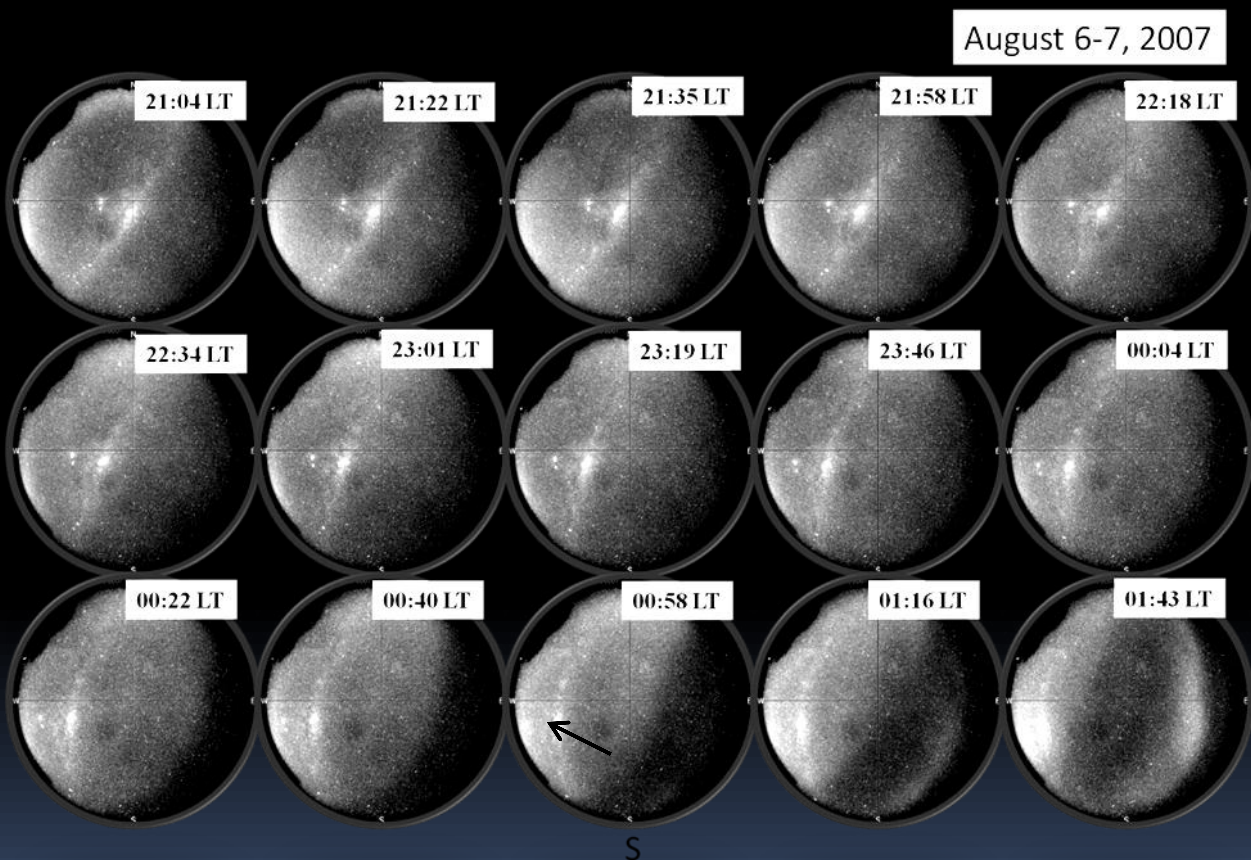

Depletions/MSTIDs Low latitude

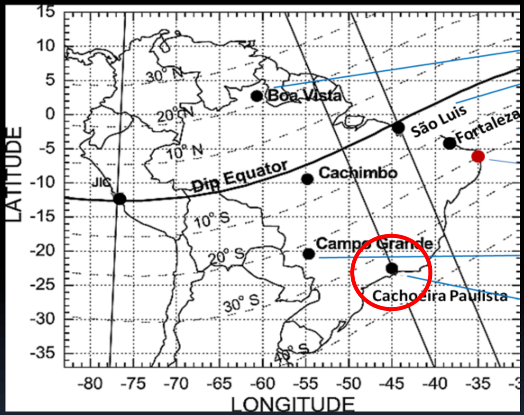

Looking at the ionosphere in the solar minimum 2007!

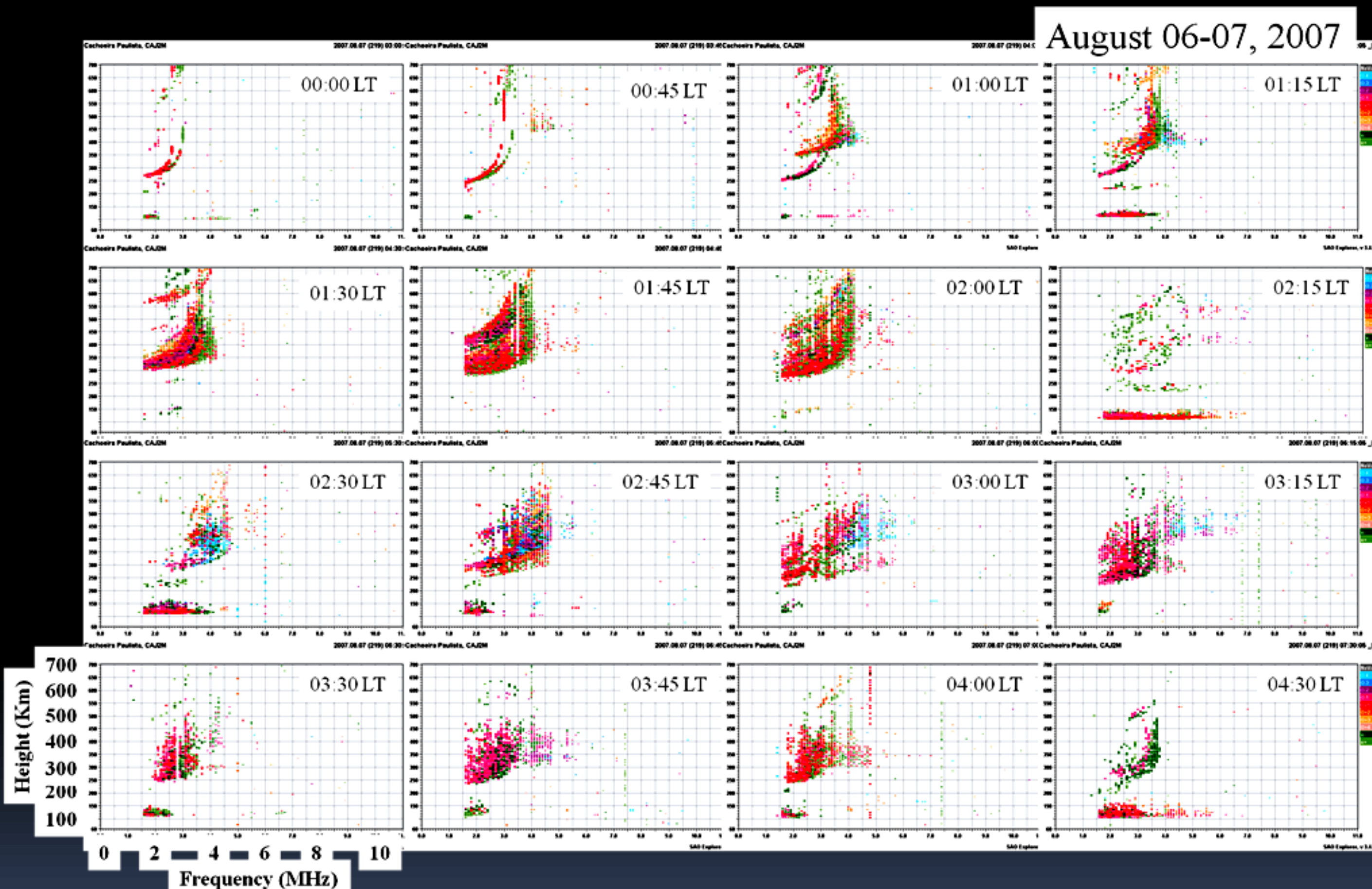

MSTIDs and spread-F/ irregularities

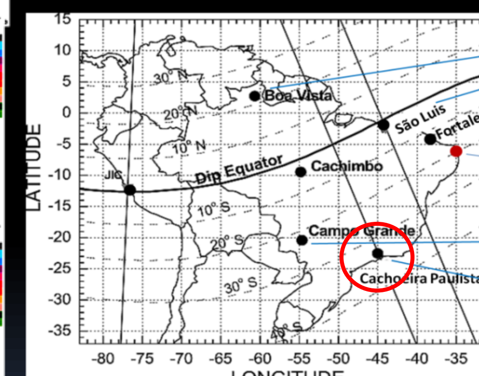

Looking at the ionosphere during the solar cycle 23/24!

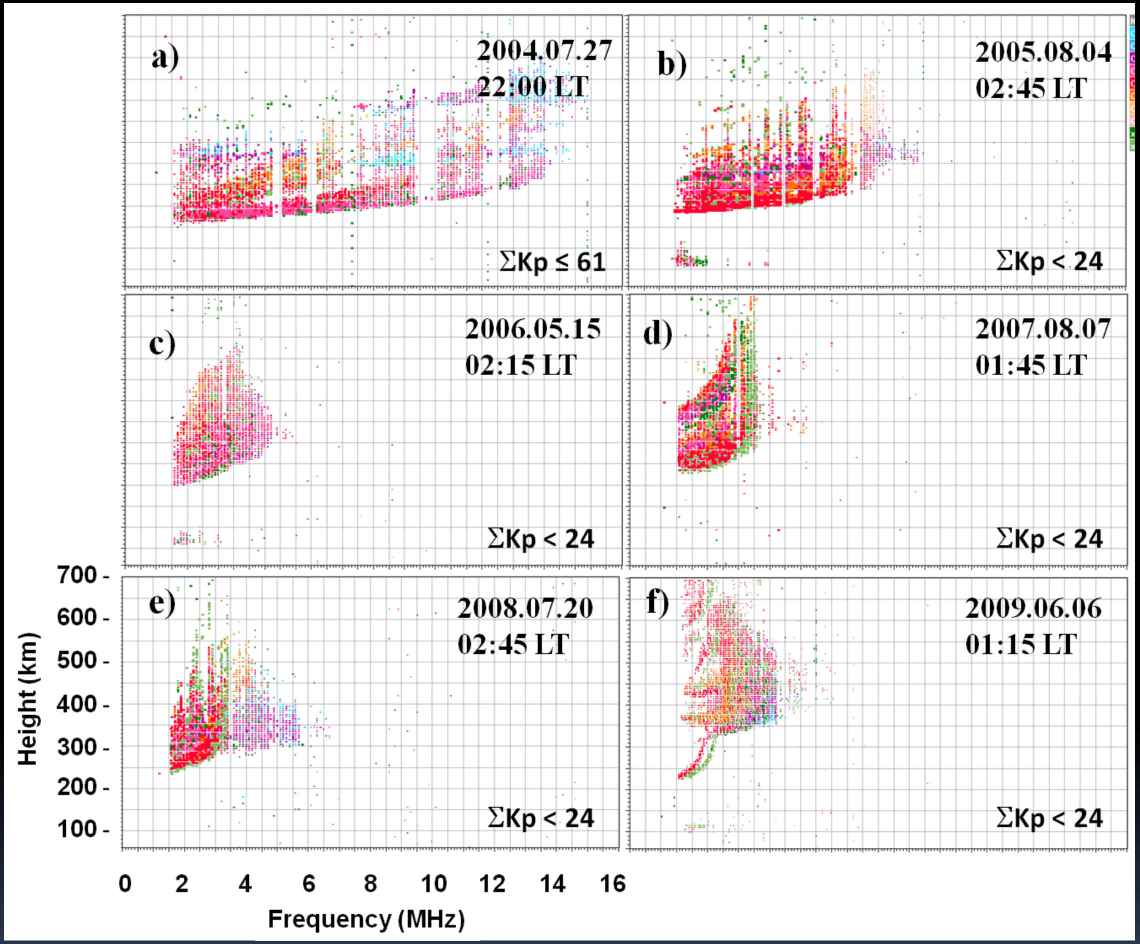

Post-Midnight irregularities

a) Plasma bubbles (disturbed night)

b) Plasma bubbles (quiet night) – rare

c) to f) meso-scale MSTIDs (quiet nights)

JUNE SOLSTICE

Low Latitude Spread-F and Solar Flux (F10.7)

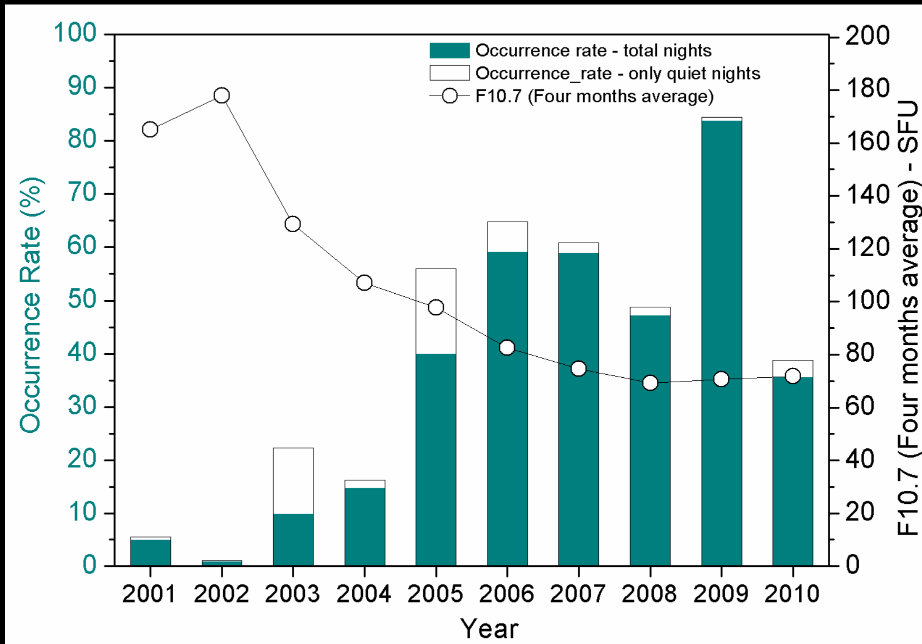

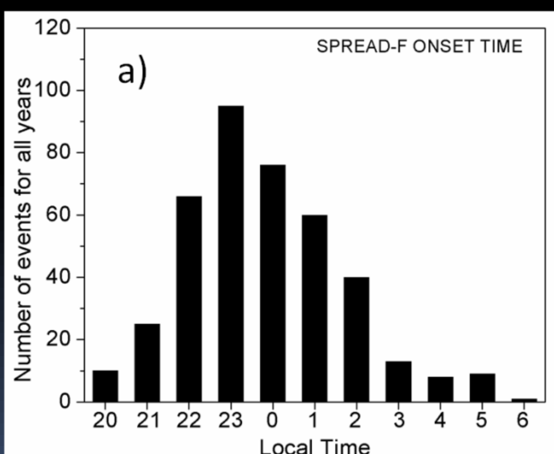

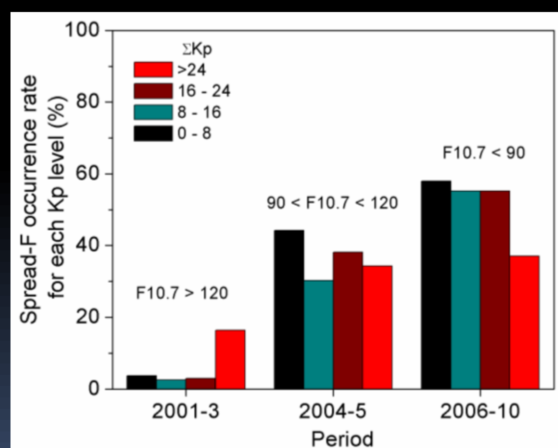

Candido et al., JGR, 2011

<u>Inverse Correlation Spread-F occurrence and Solar Flux</u>

Occurrence Peak at Solar Minimum Period

June Solstice

Pre-Midnight to Post- Midnight

Equatorial Spread-F
June solstice
2011

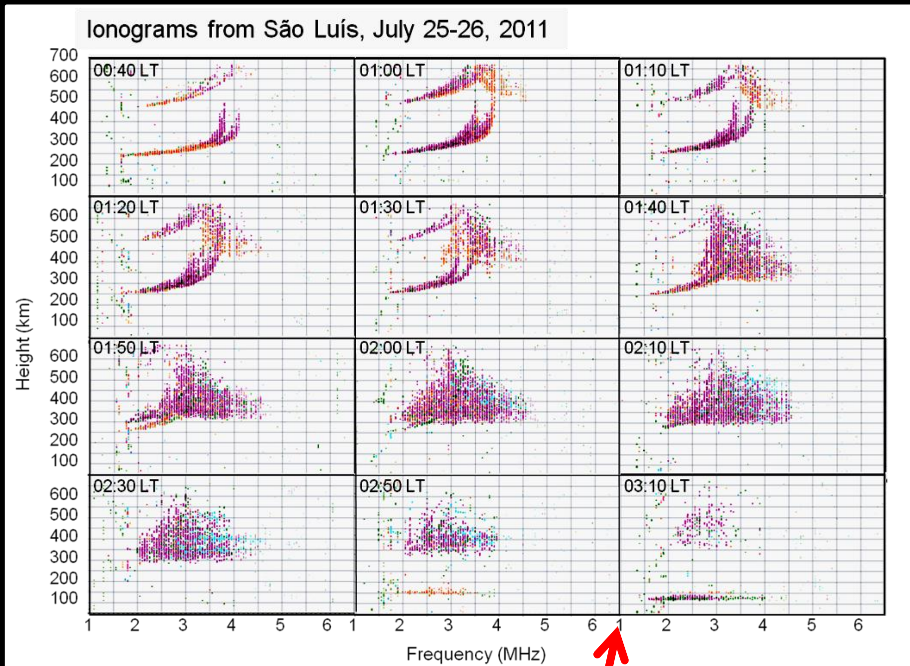

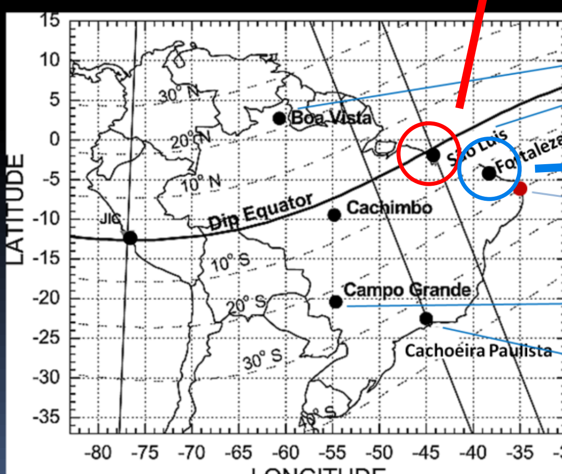

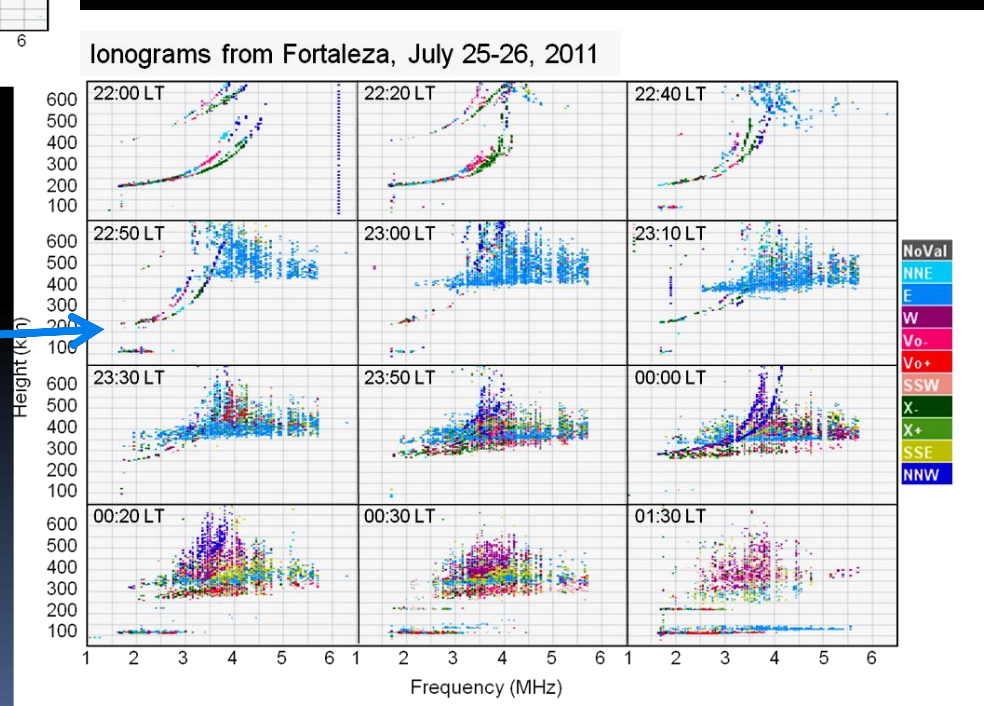

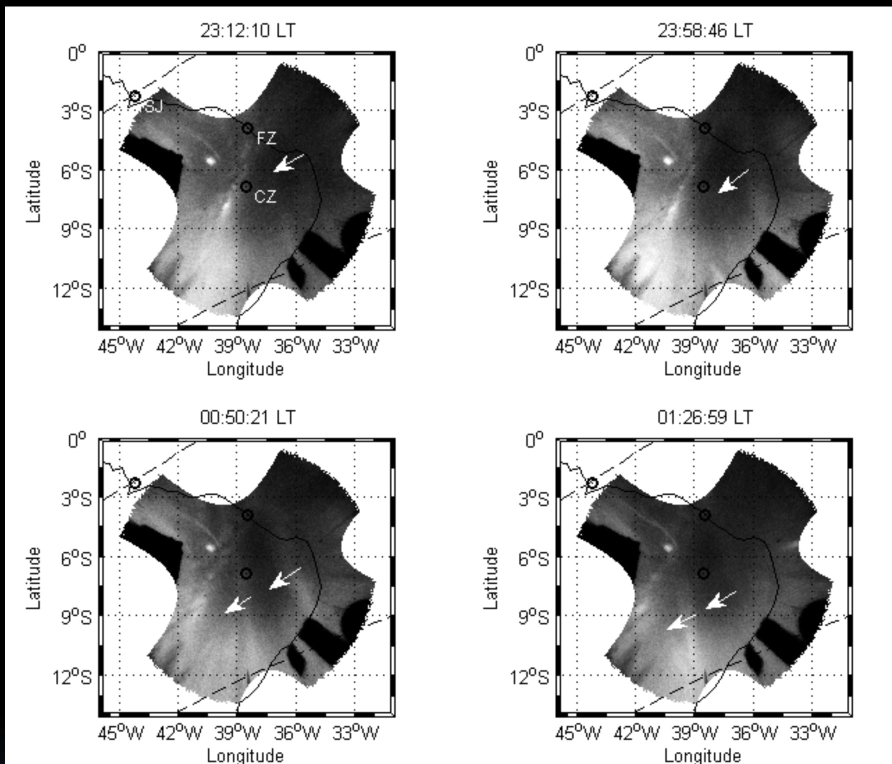

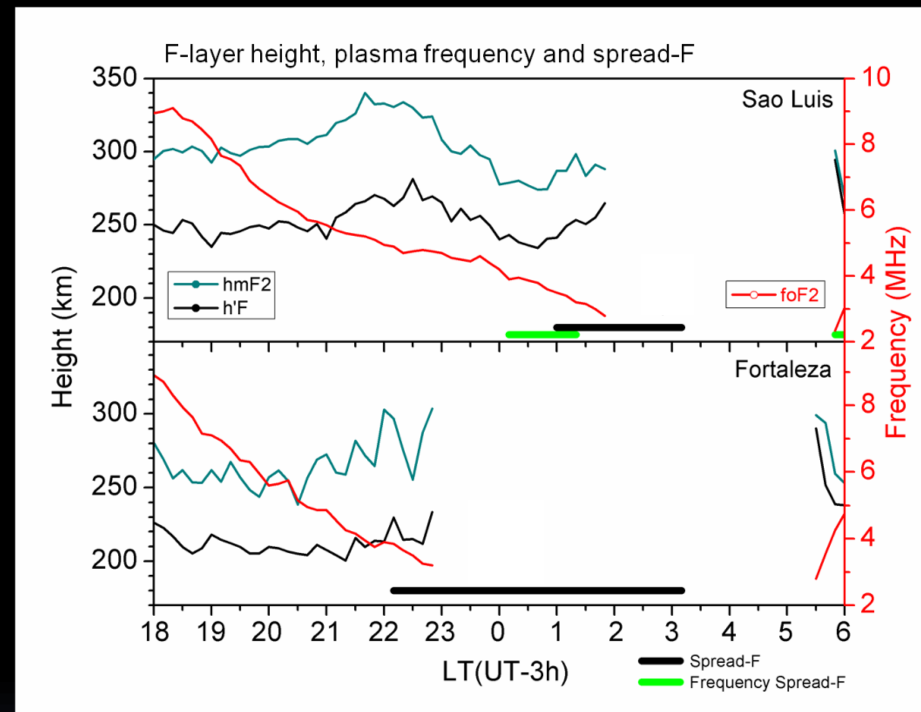

Images OI 630.0 nm
Makela (Cajazeiras, Brazil)

Ionospheric Parameters
Digisondes
São Luis (top panel)
Fortaleza (bottom panel)

Equatorial Post-Midnight irregularities 2011

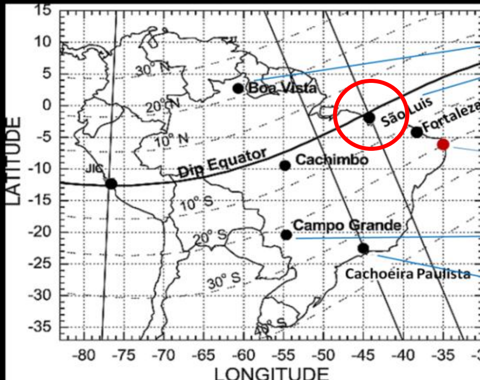

Candidoet al., JGR submitted

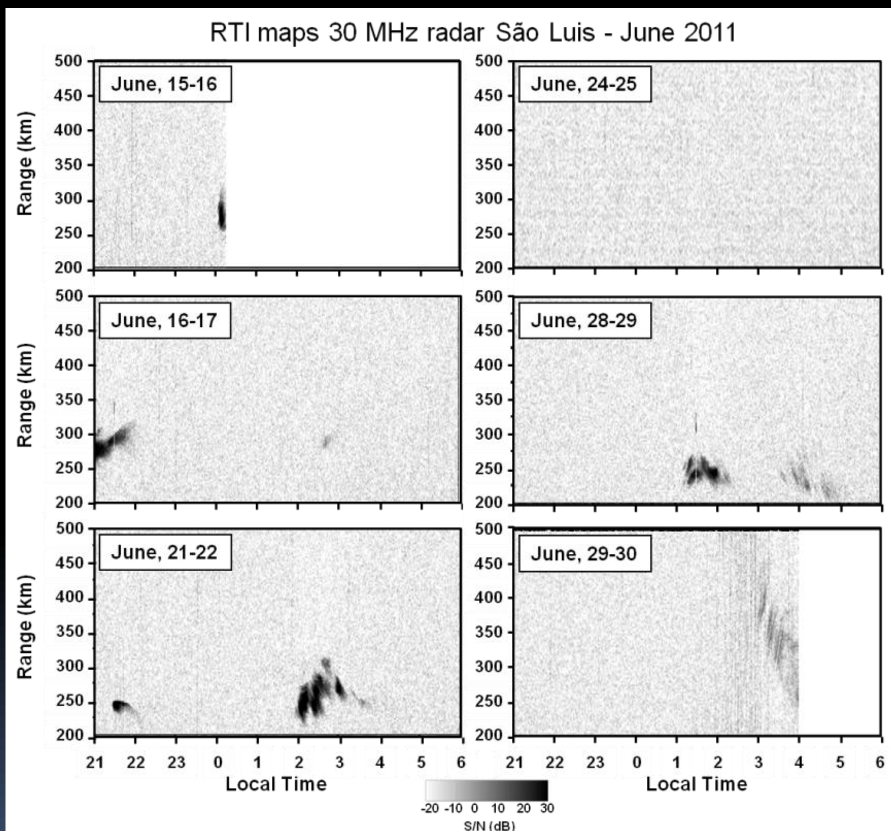

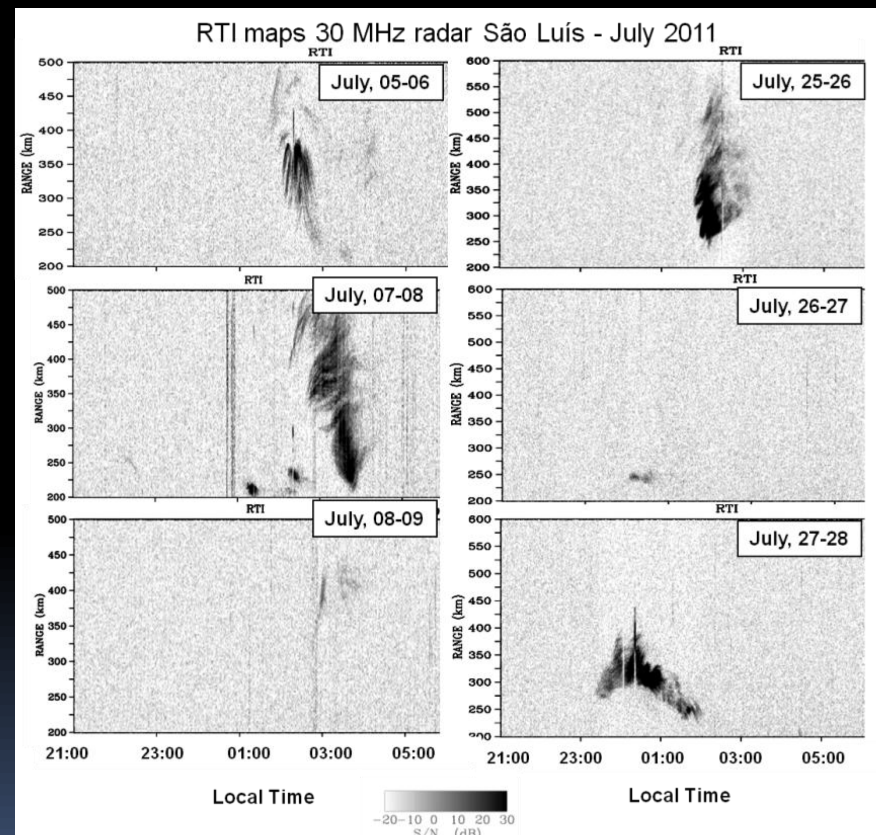

Very distinct patterns of echoes/irregularities

Equatorial Ionosphere variability

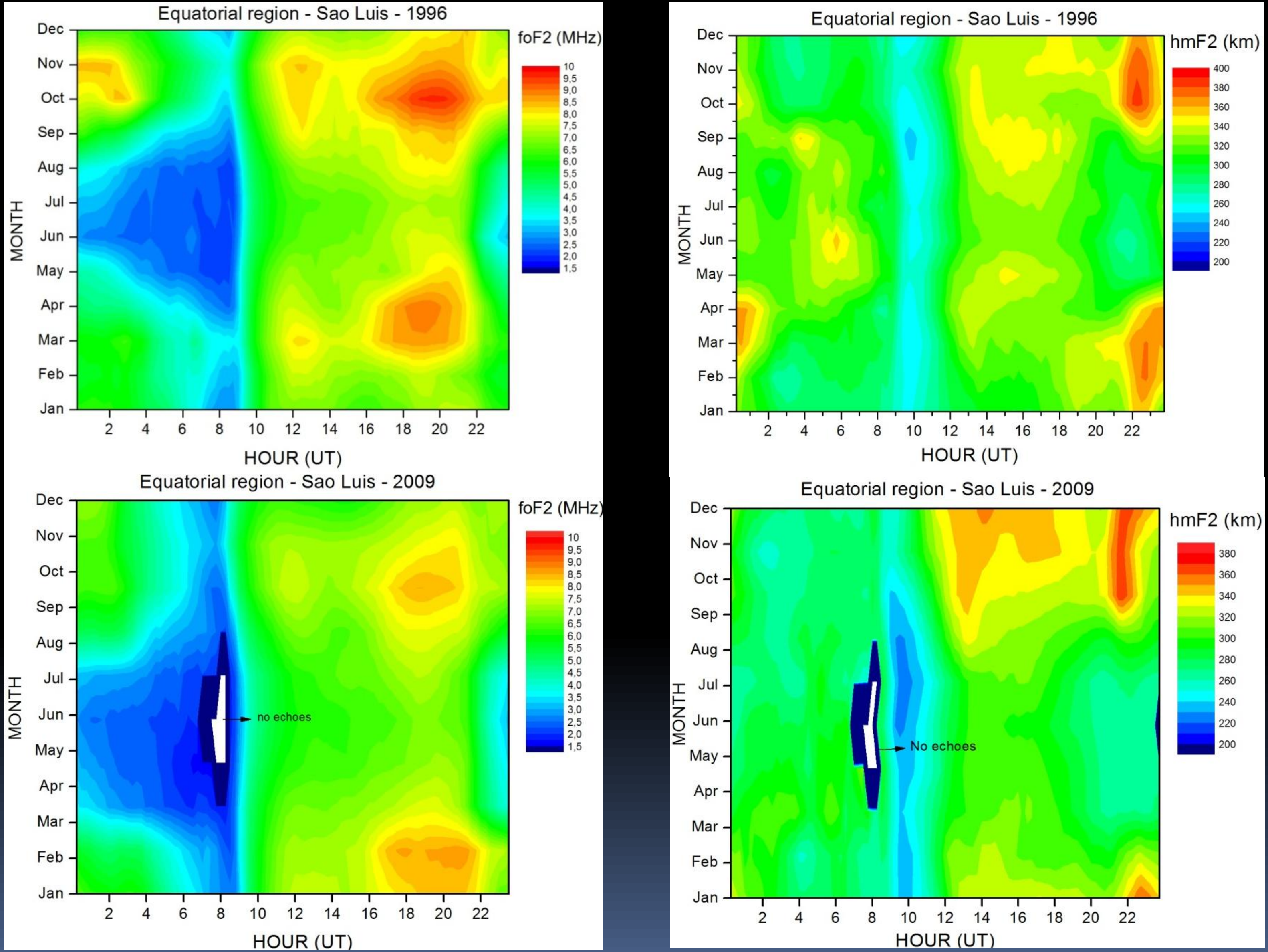

Low latitude Ionosphere variability

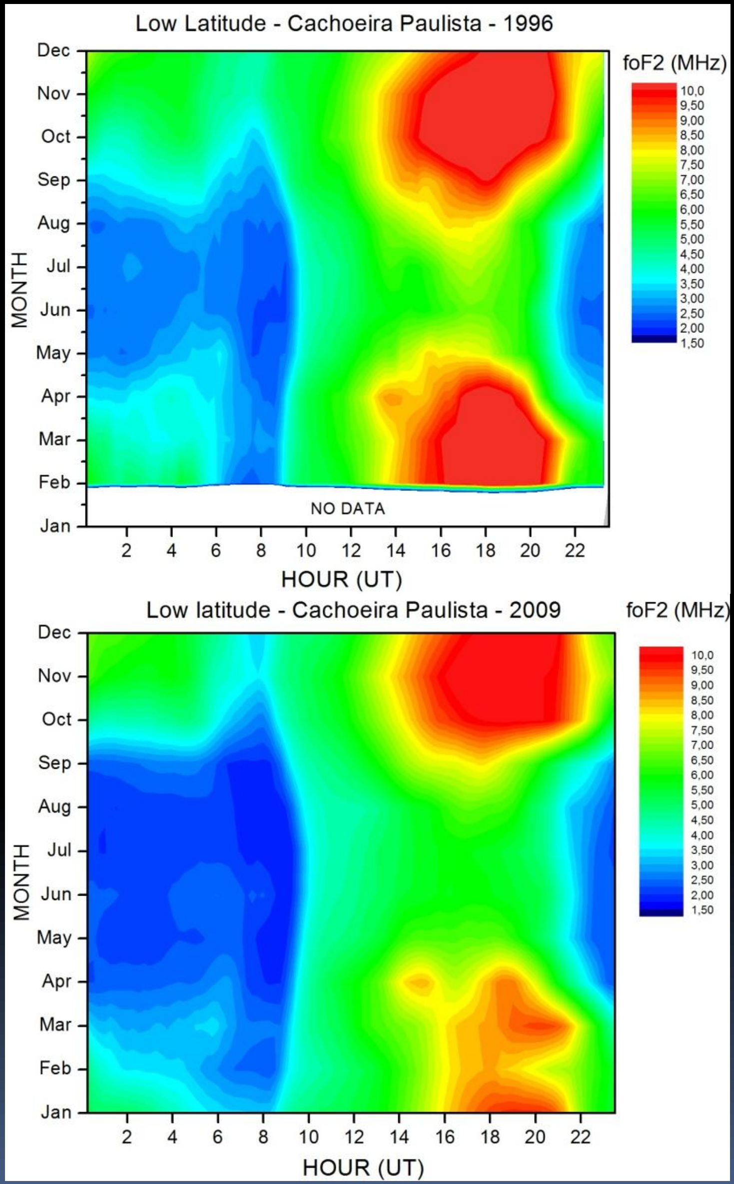

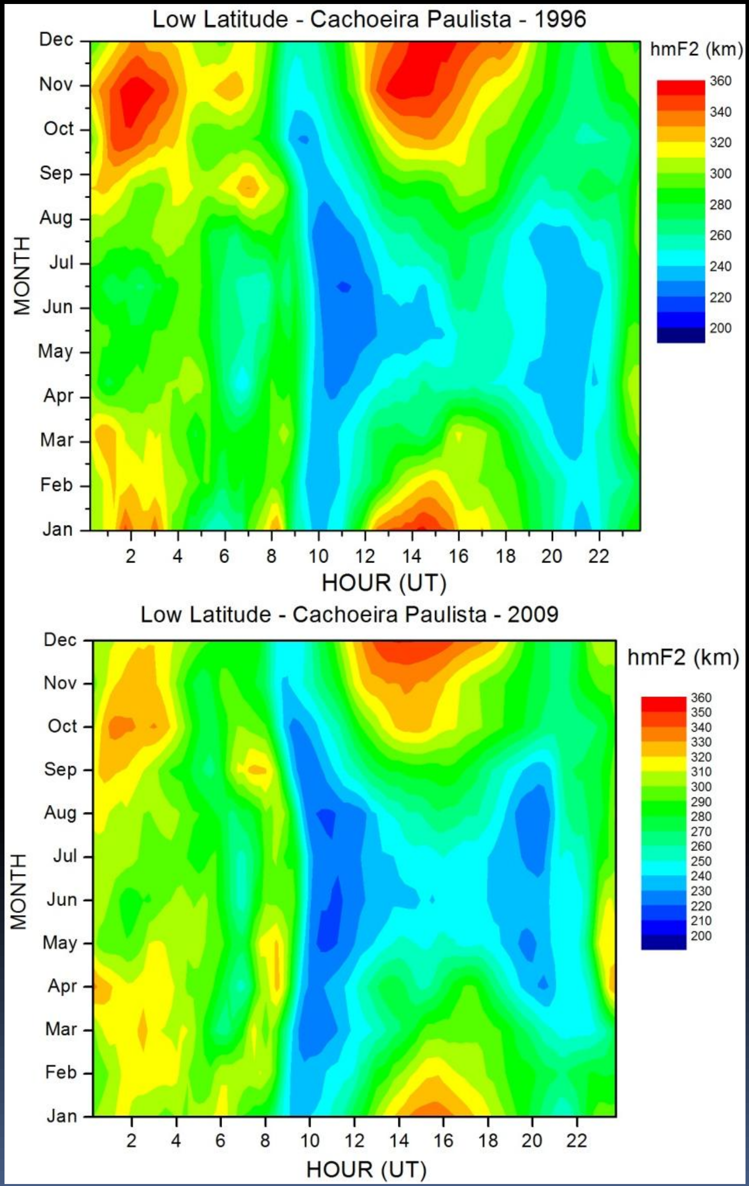

Summary

Equatorial region - Sao Luis (44.2° W, 2.33° S, dip angle: −6.9°)

• hmF2 during 2009 was lower than during 1996, both day and night except during December solstice (Summer)

• foF2 (NmF2) didn't present remarkable differences

• PRE peak: occurred earlier in 2009 than in 1996 and was higher (22 % - December Solstice and 15 % Equinox)

Low latitude region - Cachoeira paulista (23º S, 45º W,

• hmF2 and foF2 were higher in 1996 than in 2009

• High ocurrence of plasma irregularities at low latitudes probably associated with mid-latitude processes – MSTIDs

•Observation of meso-scale irregularities in both latitudes

Solar Minimum
Solar Cycle 24

Next Solar Minimum

Review

Configuration,
Calibration and/or
Location
of
instruments

Install new instruments

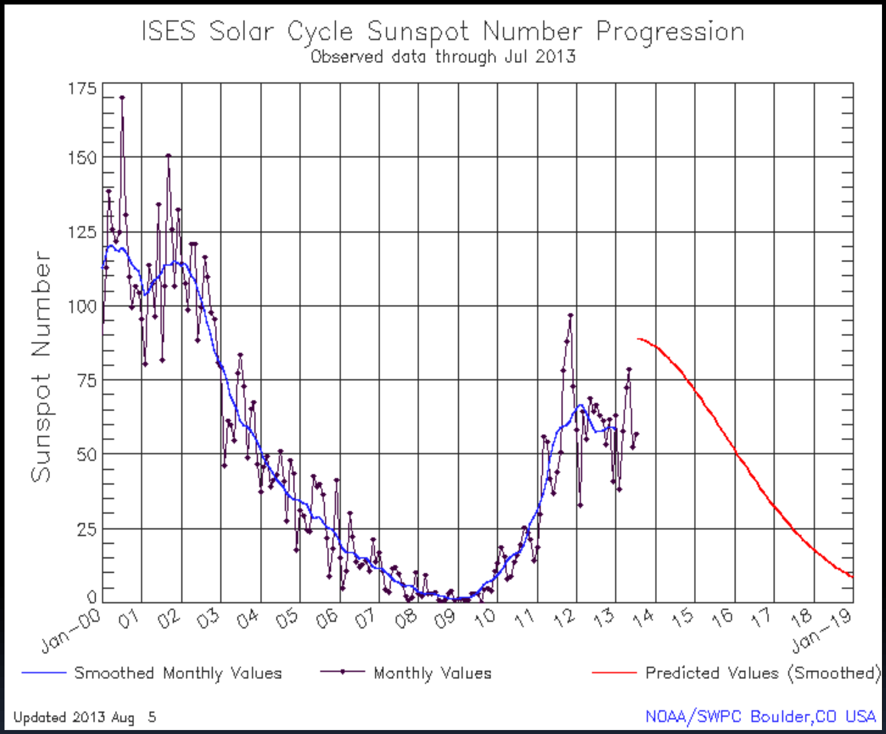

Acknowledgments

To the technical and scientific Staff of INPE – Brazil

To Conselho Nacional de Desenvolvimento Científico e Tecnológico – CNPq - for the partial financial support
Proc. 503188/2011-5

To the organizers of the Escuela de ionosonda VIPIR em Jicamarca fot eht partial financial support

To my family for the support